



The spatiotemporal properties of the Craik–O’Brien–Cornsweet effect are consistent with ‘filling-in’

M.P. Davey, T. Maddess *, M.V. Srinivasan

The Australian National University, Research School of Biological Sciences, Centre for Visual Sciences, GPO Box 475, Canberra ACT 2601, Australia

Received 4 September 1996; received in revised form 4 September 1997

Abstract

The Craik–O’Brien–Cornsweet effect (COCE) is an illusion in which luminance discontinuities give rise to illusory brightness. One hypothesised mechanism for the induction of illusory brightness is that the cortex constructs a brightness percept from edge information by a lateral ‘filling-in’ process. A requirement for the filling-in hypothesis is that ability of the illusion to form would be limited by the speed of propagation of the filling-in. The results presented here from three methods indicate that in the case of COCE gratings brightness information propagates at a fixed speed across the central visual field of about $19^\circ/\text{s}$, and across visual areas V1 or V2 at 155 or 205 (± 20) mm/s, respectively. © 1998 Elsevier Science Ltd. All rights reserved.

Keywords: Illusory brightness; Filling-in; Velocity; Lateral interactions; Craik–O’Brien–Cornsweet effect; Cortical processing; Visual cortex

1. Introduction

1.1. Illusory brightness and the Craik–O’Brien–Cornsweet effect

The Craik–O’Brien–Cornsweet effect (COCE) is a visual illusion where the perceived brightness of a region can be affected by luminance gradients or discontinuities near the enclosing edges of that region [1–3] (see Ref. [4], for review). For example, the central regions of each of the bars of the grating in Fig. 1 appear to be alternately light and dark. The intensity profile overlaid on this grating shows, however, that the central regions of each bar are in fact equally luminant. It is as though our visual system has taken the information carried by the luminance discontinuities at the edges and filled in the missing brightness between them. A COCE grating can thus appear very similar to, or even indiscriminable from, a grating consisting of an alternating series of uniformly luminant bars—a so-called square-wave grating (cf. Fig. 2, bottom).

The perceived similarity of COCE and square-wave gratings can be understood in part in terms of the

suppression of low spatial frequencies by achromatic retinal ganglion cells with receptive fields organised in a centre-surround fashion [3,5,6]. The COCE and square-

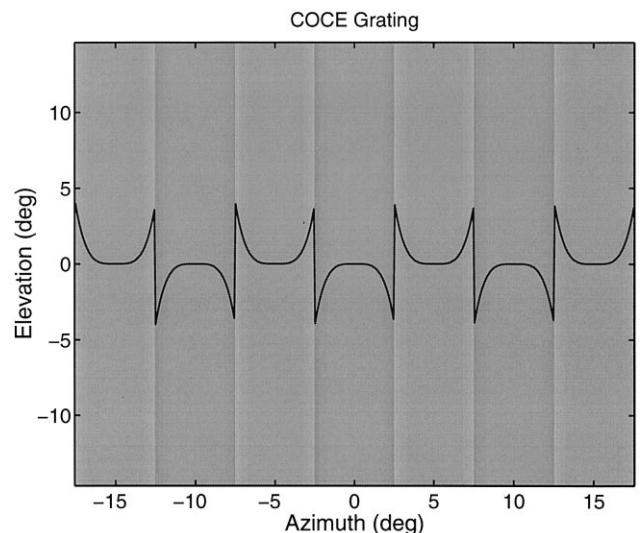


Fig. 1. A Craik–O’Brien–Cornsweet effect (COCE) grating. The intensity profile (solid scalloped line) has been overlaid on the grating. Note that despite the apparent differences in the brightness of the central regions of successive bars, the intensity of each of these regions is the same.

* Corresponding author. Fax: +61 6 2493808; e-mail: ted.maddess@anu.edu.au.

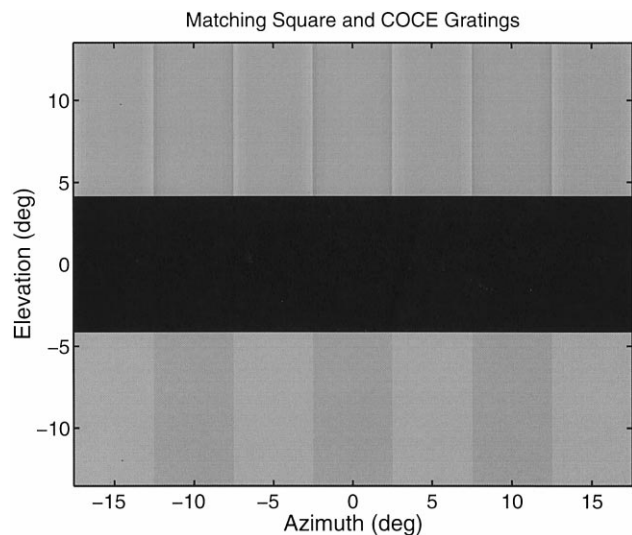


Fig. 2. Stimulus layout for Experiment 1 for matching the induced modulation of COCE gratings and square-waves. Both gratings were modulated sinusoidally in time and subjects adjusted the contrast of the square-wave grating (lower) to match the observed depth of illusory modulation in the central 1° of a COCE grating (upper).

wave patterns differ only in the lower spatial frequency region of their Fourier spectra and so the COCE and square-wave elicit similar responses from the retina. Thus retinal filtering explains why the gratings may look alike, but not why they look the way that they do. That is, how is the retinal output transformed into a percept where the brightness is filled-in?

1.2. A proposed mechanism of the COCE: 'Filling-in'

It has been hypothesised that brightness processing is mediated by a cortical filling-in process [7–9]. This filling-in hypothesis contends that brightness information spreads laterally in a cortical map representing the visual field, moving from the edges towards the middle of each grating bar. According to this hypothesis, the perceived brightness of each point in the visual field is represented by some measure of activity of the corresponding point in the cortical representation.

A filling-in process should require some finite amount of time for the brightness to spread from cortical locations corresponding to two neighbouring edges of a COCE grating into the cortical space between them. One would thus expect a cut-off temporal frequency beyond which the filling-in process would be overwhelmed: no illusory modulation of brightness over time would occur above this temporal frequency. Furthermore, this cut-off temporal frequency should increase with increasing spatial frequency, as the cortical distance over which filling-in must occur is then reduced. This hypothesis was tested in our first three experiments.

1.3. Interpretive mechanisms as alternatives to filling-in

An alternative hypothesis put forward to explain the illusory brightness in COCE gratings is that higher cortical centres compensate for retinal filtering by associating the retinal output with a percept of the pattern with filled-in brightness via an interpretive map [10,11]. According to this interpretive hypothesis, a COCE grating is perceived to be a square-wave grating at those spatial and temporal frequencies and levels of contrast where the low spatial frequency information differentiating the patterns is removed by retinal filtering. The patterns would thus become discriminable when the low spatial frequency information differentiating the two is above the contrast at which it would be independently visible [12]. At this contrast COCE patterns appear scalloped rather than square, hence the often used term 'scalloped threshold'. Sullivan and Georgeson [12] showed, however, that the induction effect can not only persist to contrasts several octaves above the threshold for seeing the missing low frequency components (on their own), but that these relatively high contrast COCE gratings can still be indiscriminable from square-waves. That is to say the scallop threshold can occur at contrasts well above the threshold at which the missing low spatial frequency components would be visible. This departure is largest at lower luminances and for contrast reversed gratings [12]. Results at higher luminances, employing temporally unmodulated COCE patterns, tend to support the original interpretive hypothesis [13–16]. Given that our gratings are temporally modulated we have sought to partially address Sullivan and Georgeson's [12] results by comparing thresholds for the visibility of the slightly different missing low spatial frequency components of our COCE gratings with the upper contrast limit at which illusory brightness induction is still observed.

2. Methods

Grating patterns were displayed on a Barco CCID 7551 monitor at a pixel resolution of 512×420 , a refresh rate of 102 Hz, and a mean luminance of 45 cd m^{-2} . The intensity levels were set with a precision of about 0.1%. Subjects viewed the gratings binocularly. The viewing distance was maintained at 60 cm with the aid of a chin rest. The gratings were composed of an odd number of vertical bars in order to ensure that one bar always lay in the middle of the display. In all tests grating contrast was modulated sinusoidally over time and subjects were required to make judgments based on any perceived modulation induced in the central portion of the COCE stripes. Fig. 1 provides an example of a COCE pattern at one extremum of the temporal modulation sequence, and demonstrates the spatial lay-

out. The spatial profile of the waveform was composed of quartic sections (Appendix A). Quartic functions were selected because the flat bases of quartic functions (Fig. 1, solid scalloped line) mean that the whole of the region over which subjects were asked to make judgements was essentially unmodulated and so any induced brightness modulation perceived in this region would be illusory. The presentation order of the stimuli was randomised in all experiments. All subjects had normal or corrected-to-normal vision. This study was conducted under protocol M881 of the Human Ethics Experimentation Committee of the Australian National University. All subjects gave informed written consent.

In Experiment 1 subjects were asked to match the depth of modulation perceived in a COCE grating to that of a square-wave grating. The stimulus layout is illustrated in Fig. 2. Both gratings had their contrasts modulated sinusoidally in time and the modulation of the gratings was synchronous. Preliminary experiments showed that the subjects had difficulty in making this judgement at a specified point; therefore the subjects were asked to consider whether brightness modulation was perceived within a circular judgement area spanning 1° in the middle of the central grating bar. No fixation points were provided as such marks may have provided subjects with a reference point of fixed brightness, thereby confounding the measures of illusory brightness. The size and location of this area was demonstrated to the subjects before the experiments. The horizontal central stripe (Fig. 2) was black and wide enough to prevent grating induction [17] across this band. A modified binary search was used in our first experiment to determine the contrast match [18]. The method of adjustment was used for all subsequent experiments. Four subjects participated in Experiment 1, two of these subjects were naive as to the purpose of the experiments.

In Experiment 2 subjects were presented with modulated COCE gratings, initially having contrast 0.1, and they were asked to adjust the contrast to find a level sufficient to induce modulation in the central 1° of the central stripe of each COCE pattern. The stimulus was presented over the whole monitor, as in Fig. 1 (but without the intensity profile). The same four subjects as those in Experiment 1 were used. The location of the 1° region was illustrated for the subjects before the experiments.

In Experiment 3, the subjects varied the temporal frequency of a contrast 0.1 COCE grating to determine the maximum temporal frequency at which temporal brightness modulation was perceived in the central 1° of the middle bar. This experiment was less time consuming than the previous two. Temporal frequency thresholds were determined at seven spatial frequencies ranging between 0.042 and 0.212 cd: a super-set of those used in Experiments 1 and 2. Seven subjects performed this task, each between two and four times.

Experiment 4 incorporated a waveform constructed by subtracting the COCE wave-form from a square-wave grating of equal contrast and spatial frequency; this grating will be termed the difference grating. For each spatial frequency the presentation temporal frequency was that obtained in Experiment 3 (on completing Experiment 3 each subject proceeded immediately to Experiment 4). Subjects varied the contrast of the difference grating to find the minimum contrast at which temporal modulation was perceived in the centre of the middle bar. The difference grating is very similar to a sine wave: the amplitude of the fundamental Fourier component of the difference grating is four times as large as the sum of the amplitudes of all of the other components and at threshold the difference grating has the appearance of a sinusoidal grating. Thus the weak higher harmonics mean that, at the threshold for the difference grating, these higher harmonics are sub-threshold and do not contribute to the percept near threshold.

Multiple regression analysis was conducted with SPSS (SPSS International BV, Gorinchen, The Netherlands). For each data set an attempt was made to see if separate effects for subject and spatial frequency could be found and whether any such model was significantly different from a model containing spatial frequency alone. Model significance and comparison of models were determined by *F*-tests. Fitting such models meant that while the mean thresholds may have varied between subjects, probably reflecting some subjectivity in the judgement of brightness modulation, it was possible to estimate the slope of the dependence of critical temporal frequency upon spatial frequency. A fixed slope significantly greater than 0 indicates a finite spreading velocity for the tested induction effect.

3. Results

3.1. Experiment 1: Matching square-wave gratings to COCE gratings

The means of psychometric functions for four subjects are shown in Fig. 3. The functions show the amount of square-wave contrast required to match the modulation of the COCE grating at each temporal frequency, for each of three spatial frequencies. The principle finding was that induced modulation was stronger and persisted to higher temporal frequencies for higher spatial frequencies. The dashed horizontal line in Fig. 1 represents 70% of the distance from the mean to the contrast values obtained at 0 Hz and the basal level (actually measured out to 16 Hz but not shown). As will be evident the parallel nature of the psychometric curves means that the exact level chosen to compare results for different gratings does not mat-

ter since it is the distance between these functions which determines the slope of the relation between the criterion temporal frequency and the test spatial frequency.

For each function two continuous curves are shown through the data points, one being the straight line or trapezoidal spline and the smoother curve being a thin plate spline [19]. The two interpolation methods are shown to illustrate that either method provides much the same answer. Having no parametric model to fit to the functions we simply took the interpolated temporal frequencies corresponding to the 70% level from the trapezoidal spline values (e.g. *, Fig. 3) for further analysis. The values used for regression analysis (Section 2) were taken from individual interpolated psychometric functions rather than those obtained from the mean psychometric curves. These resulting temporal frequency values were then plotted against their respective spatial frequencies, the means being shown in Fig. 4 (*). No significant subject effect could be fitted and so a simple regression on spatial frequency is shown (dashed-dot line). The slope of this line (\pm S.E.), $11.24 \pm 3.27^\circ/\text{s}$, was significantly different from 0 ($P = 0.0065$), such a relationship is consistent with a fixed speed of spreading of brightness information from the edges of the COCE grating towards the centre of each stripe.

3.2. Experiment 2: Contrast for modulation induction

Here subjects adjusted the contrast of COCE gratings, contrast modulated at various temporal frequencies, to find the minimum contrast at which illusory brightness modulation occurred. As temporal frequency

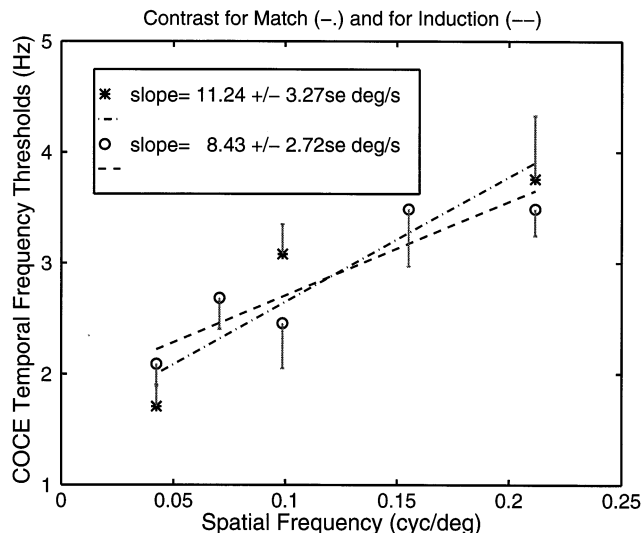


Fig. 4. Data from Experiment 1, square-wave contrast to match COCE modulation (—, *); and Experiment 2, contrast for induction (---, O). Both are presented as the temporal frequencies to achieve a criterion effect (see text). The data are in reasonable agreement and both slopes are significantly different from 0 indicating that brightness information derived from the edges present in the COCE gratings propagates at a finite speed. To minimise clutter either the upper or the lower se are presented for each mean data point.

increased subjects' behaviour was to attempt to use higher contrasts to induce a modulation. A thin plate spline [19] (cf. Fig. 3) was used to interpolate the data obtained for each spatial frequency to find the temporal frequency which would have required a contrast of 0.1 to just induce modulation. This procedure also provided data which could be compared more directly with that obtained in Experiments 1 and 3 which employed contrast 0.1 COCE gratings. The resulting data were fitted with a multiple regression (Section 2). A relatively significant subject effect was found ($P = 0.054$) and the independent effect of spatial frequency provided a slope of $8.43 \pm 2.72^\circ/\text{s}$ ($P = 0.0074$). Since the significance of the subject effect was marginal we also report that without fitting the independent effect of subject the estimated slope was $8.43 \pm 3.17^\circ/\text{s}$ ($P = 0.016$).

3.3. Experiment 3: The COCE temporal frequency threshold

The mean of all results for the COCE temporal frequency threshold is shown in Fig. 5. A multiple regression indicated that there was a significant subject-wise effect, $F(6,42) = 25$, $P < 0.00005$. As in Experiments 1 and 2 the temporal frequency for an induction effect increased with increasing spatial frequency: $F(1,41) = 132$, $P < 0.00005$, the resulting slope of $9.56 \pm 0.83^\circ/\text{s}$ being highly significantly different from 0 ($P < 0.00005$). The fitted lines from Fig. 4 are shown for comparison: the vertical shift of those lines in part

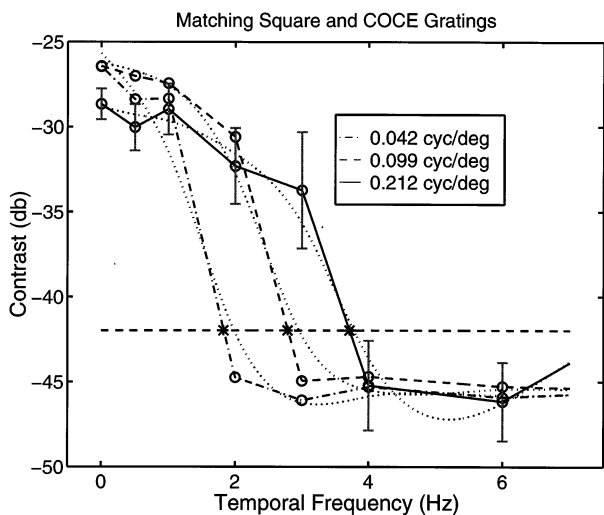


Fig. 3. Psychometric functions for Experiment 1 showing the average square-wave contrasts used to match the modulation seen in the COCE gratings. Error bars are standard errors and are only shown for the data for the 0.212 cd COCE grating. Errors for the other two curves are similar but are not shown to reduce clutter.

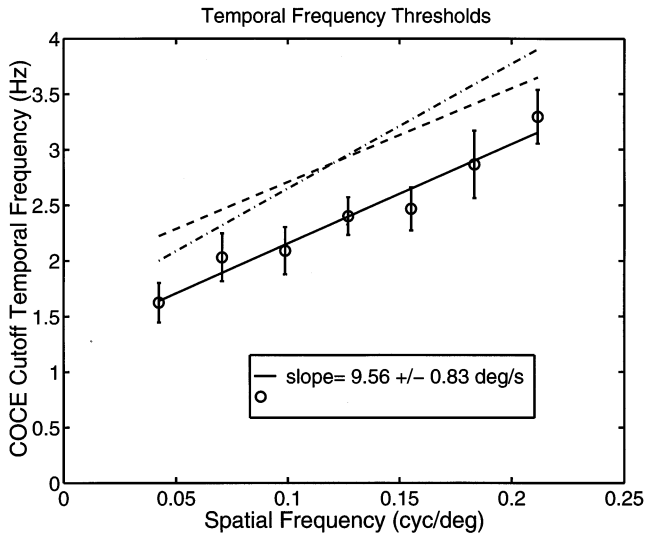


Fig. 5. Data from Experiment 3, showing the cut-off temporal frequency for the COCE as a function of spatial frequency. This figure presents the mean of 19 data sets from seven subjects, following correction for an independent subject-wise effect (Section 2). The fitted lines from Experiments 1 and 2 are reproduced here for comparison. The error bars are S.E.

reflects the fact that the seven subjects of Experiment 4 were a super-set of those used in Experiments 1 and 2.

3.4. Experiment 4: The contrast threshold for the difference grating

Fig. 6 shows a comparison of the threshold for COCE-induced illusory brightness with visibility

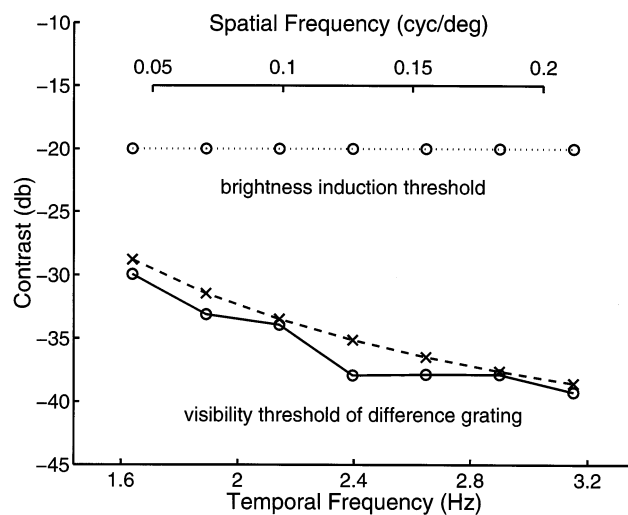


Fig. 6. Comparison of spatiotemporal thresholds for COCE-induced illusory brightness with visibility thresholds for corresponding difference gratings (solid line, O). Brightness induction occurs for between 2 and 4 octaves of contrast above the threshold for seeing the missing difference component (dotted line, O). The thresholds for the difference grating are essentially the same as those expected for the fundamental alone (dashed, x), based on the data of Ref. [20].

Table 1

Speeds of propagation of induced brightness using different methods

Experiment	Propagation speed (\pm S.E.) ($^{\circ}$ /s)	No. subjects
Contrast matching	22.44 ± 6.54	4
Contrast for induction	16.86 ± 5.44	4
Temporal frequency threshold	19.32 ± 1.55	7
Rossi and Paradiso [21]	11.33 ± 2.23	4

thresholds for corresponding difference gratings. The dual abscissa reflects the fact that the temporal frequency thresholds from Fig. 5 were used to determine the presentation temporal frequency for each spatial frequency. The fact that the illusory brightness threshold line is higher than the line of threshold for the difference grating shows that there is still induction of brightness even at contrast levels well above those where the difference grating becomes visible. It is important to state that near threshold our difference patterns appear as sinusoids. This is to be expected because the higher spatial harmonics contained in the difference pattern are less visible than those in a square-wave, and so are invisible at the threshold for the fundamental. That only the fundamental was visible is supported by the curve plotted just above our data in Fig. 6. The curve represents the predicted thresholds for the fundamental based on the spatiotemporal threshold function published by Kelly [20].

4. Discussion

As explained in Section 1, the filling-in hypothesis predicts that there should exist a temporal frequency cut-off for the perception of COCE-induced illusory brightness, and that this temporal frequency should increase with increasing spatial frequency. The results shown in Figs. 3 and 4 are thus consistent with the filling-in hypothesis or at least some process requiring the lateral propagation of information about the brightness of edges in the COCE gratings. The slopes of these functions, although derived from different methods, are in good agreement as summarised in Table 1.

The values reported in Table 1 represent speeds of propagation of induced brightness which are twice the slopes reported so far. This doubling corrects for the fact that the brightness induction proceeds across 1/4 of a cycle (i.e. 1/2 of a bar from its edge to its middle) and that two inductions occur per temporal modulation. Also presented in Table 1 are values based on the data of Rossi and Paradiso [21]. Those authors examined the

induction of brightness modulation in neutral grey regions placed between modulated rectangular bars. We have extracted the raw data from their paper (from their Fig. 2) and performed the same regression analysis as employed for the data presented in Figs. 3 and 4. Placing 95% confidence limits on Rossi and Paradiso's data allows a range of propagation speeds of $11.33 \pm 7.10^\circ/\text{s}$, thus permitting an upper limit of $18.43^\circ/\text{s}$: overlapping with the lower bound (at 95% confidence) of our most accurate method at $15.53^\circ/\text{s}$ ($19.32 - 3.79$, $df = 6$), and close to our grand mean of $19.52^\circ/\text{s}$. Thus, four independent measures, derived from 11 subjects, in two labs, all suggest a brightness induction propagation speed of about $19^\circ/\text{s}$ within the central 1° of the visual field.

Fig. 6 compares the contrast threshold for visible brightness modulation in the difference grating to the threshold for COCE-induced illusory brightness. Note that illusory brightness does not fail completely until the contrast is well above that required to see the difference grating independently. A similar effect was also demonstrated by Sullivan and Georgeson [12]. Those authors used so-called missing fundamental gratings, i.e. square-waves with their fundamental removed. They showed that their COCE gratings could appear completely filled-in—i.e. to look exactly like a square-wave pattern—at contrasts at which the missing fundamental Fourier component would be seven times stronger than threshold if presented on its own.

Their results pose problems for the basic interpretive hypothesis: while the interpretive hypothesis accounts well for the appearance of missing fundamental gratings below the threshold for seeing the fundamental it does not account for brightness induction above the threshold for seeing the missing component. Burr [15] demonstrated that brightness appearance of high contrast COCE patterns is not predicted by the basic interpretive hypothesis, and also that noise versions of COCE patterns violate the basic interpretive model, given their high spatial frequency content. Dooley and Greenfield [22] demonstrated that a nonlinear contrast gain control operating on spatial frequencies below 1 cd is required to extend the interpretive hypothesis to suprathreshold contrasts. Moulden and Kingdom [23] have, however, extended the interpretive hypothesis in a way which can account for some of the additional brightness induction.

Our results with the difference gratings do not represent a falsification of the interpretive hypothesis but do support Sullivan and Georgeson's [12] findings and the notion that the original interpretive hypothesis may be an incomplete theory [15,22]. Our results could in fact support more sophisticated versions of the interpretive hypothesis where the propagation of edge brightness information is required for the interpretive hypothesis. For example the basis of the interpretive hypothesis is

that the Fourier components of the COCE pattern are recognised as being square-wave-like, and the lack of lower spatial frequencies is also in effect recognised. If these recognition processes were spatial frequency dependent, say requiring communication between distant cortical cells, then such an interpretive mechanism would have a brightness information propagation speed.

Assuming for the moment that some form of propagation of brightness information does mediate COCE-induced illusory brightness perception, there is good reason to believe that such a process occurs in the visual cortex [7,9,24–26]. Whether that process represents filling-in or some other process is immaterial to the present discussion. Whatever the exact process it is possible to use the COCE temporal frequency cut-off as a function of the spatial frequency (Fig. 5) to derive a theoretical estimate of the propagation velocity in terms of millimetres of cortex per second. To do this, we estimate the time taken for the filling-in process to spread from one of the flanking edges of the COCE grating to the boundary of the subject's inspection area. The corresponding cortical distance can be determined after taking into account the cortical magnification function. We make the approximation that the brightness signal must travel at least to the edge of the inspection area within one half-cycle of the contrast-reversal; that is, before the reversal of the edge contrast that gave rise to the brightness signal. The cut-off temporal frequency f_t is related to the spatial frequency f_s by Equation 1. The derivation is given in the Appendix A. v represents the cortical propagation velocity in mm/s, A , B and C are constants determined for V1 to V4 by Sereno et al. [27] in fitting the human cortical magnification factor M to an equation of the form $M(r) = A(r + B)^{-C}$, where M is in mm° . The diameter of the central judgement area, j , was 1° .

$$f_t = \frac{v(1 - C)}{2A \left[\left(\frac{1}{4f_s} + B \right)^{1-C} - \left(\frac{j}{2} + B \right)^{1-C} \right]} \quad (1)$$

Fig. 7(a) shows this equation fitted to the data in Fig. 5 assuming that brightness information propagation occurs in V1. The fit is best for a cortical propagation velocity of around 155 ± 15 mm/s. Note that the only variable available for fitting Eq. (1) to the data is the cortical propagation velocity v . It is encouraging that this one variable may be set such that the resultant theoretical relationship fits the shape, slope and vertical displacement of the data.

It is possible that the propagation effect could occur in a visual area other than V1 [7]. Electrophysiological experiments suggest that illusory contours [28,29] may be first defined at the level of V2 [30–32]. Perhaps filling-in of contours and filling-in of brightness could occur in the same cortical area. Fig. 7(b) shows the data

as they compare to a theoretical plot where the values of A , B and C were determined for V2 by Sereno et al. [27]. The fitted cortical propagation velocity is 205 ± 20 mm/s.

4.1. Comparison of results with physiological data

The most likely basis for filling-in seems to be the spread of activity through excitatory connections in the cortex [7,8,33,34]. In this context, it is useful to compare the velocities of propagation estimated here with those observed for epileptiform discharges. A similar comparison between the spread of brightness information and of the propagation of epileptiform discharges has been made by Paradiso and Nakayama [35]. An epileptiform discharge is a synchronous depolarisation of a large number of neighbouring neurones [36,37]. The cortex contains an extensive network of neurones linked through excitatory connections [38–42]. It is likely that these connections are the mechanism by which an epileptiform discharge propagates to other neural areas [43,44].

Chervin et al. [44] found velocities for propagation of epileptiform discharges which ranged from 63 to 88 mm/s in slices of the primary visual cortex of the rat and the cat, and of the primary somatosensory cortex of the rat. Goldensohn and Salazar [45] obtained a value of 250 mm/s in an *in vivo* preparation of cat sensorimotor cortex. It has been suggested that the penicillin treatment used by Goldensohn and Salazar [45] may have influenced the propagation of the discharges, and that the method did not control for propagation through tissues beneath the neocortex [44]. Gutnick and Wadman [46] reported values ranging from 20 to 150 mm/s for the propagation of epileptiform discharges across slices of the parietal cortex of the guinea pig. Wadman and Gutnick [47] reported a

velocity of 70 mm/s in rat parietal cortex. The velocities estimated by this study are 155 or 205 mm/s, depending upon whether we assume that propagation occurs in V1 or V2. These values correspond fairly well with the physiology after allowing for differences between in soma sizes and axon diameters in the visual cortices of humans and the laboratory animals.

4.2. Comparison of results with psychophysical data

Paradiso and Nakayama [35] reported results consistent with a filling-in model for non-illusory brightness. Their estimates for the propagation velocity of filling-in were in the range of 150–400 mm/s. Studies of the critical temporal frequencies for induced brightness [21,48] are similar to those determined here for illusory brightness (Fig. 6). Rossi and Paradiso [21] found that the cut-off temporal frequency for brightness induced between solid stripes increases with spatial frequency. The relationship between cut-off temporal frequency threshold and spatial frequency as reported by Rossi and Paradiso [21] varies greatly between subjects for spatial frequencies above 1 cd. Our subjects reported having great difficulty in restricting their attention to the central area of each bar at spatial frequencies above 0.4 cd, a complaint consistent with the large variation between subjects noted at these spatial frequencies. Perhaps the results in Rossi and Paradiso [21] reflect the same difficulty at high spatial frequencies. In any case, the overall similarity between our findings and theirs (Table 1) suggests that similar processes may underlie the phenomenon of brightness induction in simultaneous contrast and the filling-in that is observed in the COCE illusion. Given that the retina deletes the low spatial-frequency content of a square-wave grating and makes the stimulus almost indistinguishable from a COCE profile, it quite possible that the two phenomena reflect the same kind of processing at the cortical level.

Rossi and Paradiso [21] did not use their data from their Fig. 2 to estimate the velocity of brightness induction. Instead they employed another method which produced estimates around $160 \pm 20^\circ/\text{s}$. They estimated the filling-in velocity by examining phase differences between real and induced brightness modulation. It has been proposed that a filling-in process may underlie the processing not only of illusory or induced brightness but also real brightness [9]. This suggestion is supported by psychophysical results [35,49]. These models of filling-in predict that there would be little if any phase differences between real and induced brightness; therefore it does not seem that any such phase differences observed can be used to estimate the filling-in velocity. Moreover, a filling-in velocity of 140–180°/s requires temporal frequency thresholds ranging from 10 to 640 Hz over the spatial frequencies from 0.03 to 2 cd examined by those authors. Inspection of Rossi and

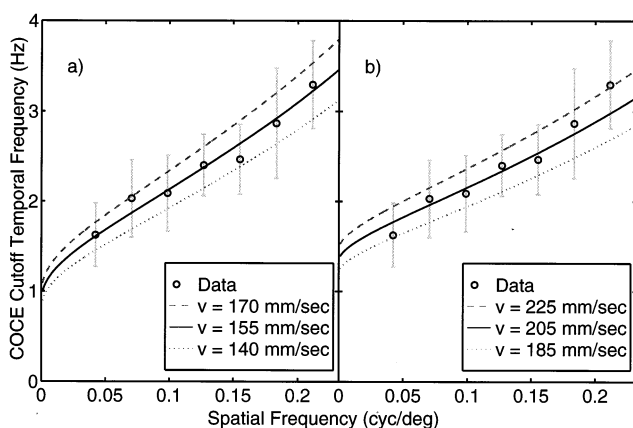


Fig. 7. Comparison of cut-off temporal frequencies measured for the COCE with theoretically predicted values, assuming that filling-in takes place in V1 (a) or V2 (b). The error bars represent 95% confidence intervals.

Paradiso's [21] other data indicate that these cut-off frequencies range from 0.7 to 5 Hz over the same spatial frequency range (their Fig. 2) and thus predict propagation velocities around $10^\circ/\text{s}$ (e.g. Table 1).

5. Conclusion

Our results indicate that a fixed cortical propagation velocity of brightness information explains the appearance of COCE gratings across a range of spatial and temporal frequencies. The results are thus consistent with a 'filling-in' process mediating COCE-induced illusory brightness. The results are inconsistent with the hypothesis of a simple interpretive mechanism where the illusory brightness occurs only when the difference between a COCE pattern and a square-wave pattern is not independently visible. It is not possible, however, to rule out all possible interpretive mechanisms. The temporal characteristics of COCE-induced illusory brightness are similar to those of induced brightness, consistent with the suggestion that propagation of brightness information from edges underlies both effects.

Acknowledgements

We thank A.C. James for contributions to the presentation software, and a reviewer for valuable comments.

Appendix A

A.1. The COCE intensity waveform

The spatial dependence of the intensity of the COCE is given here for one extremum in the temporal cycle of the COCE. $I(x)$ is the intensity and $\Delta I/\bar{I}$ is the Michelson contrast, ΔI being the maximum departure from the mean intensity \bar{I} . This sample profile has a spatial frequency of $1/2\pi$ for simplicity; it is scaled to various spatial frequencies in the experiments described here. Other COCE waveforms have been used, notably the 'missing fundamental' form used by Sullivan and Georgeson [12]. The waveform described here was used in preference to other COCE waveforms due to the existence of a broad region in the middle of each bar which exhibited negligible real modulation in intensity: any brightness modulation observed there was therefore illusory.

$$I(x) = \bar{I} + \frac{\Delta I}{\bar{I}} \left(\frac{\pi}{2}\right)^{-4} \left(x \bmod \pi - \frac{\pi}{2}\right)^4 \operatorname{sgn}(\pi - x \bmod 2\pi) \quad (\text{A1})$$

$$\text{where } \operatorname{sgn}(q) = \begin{cases} +1 & \text{for } q \geq 0 \\ -1 & \text{for } q < 0 \end{cases}$$

A.2. The cut-off temporal frequency as a function of spatial frequency

The cortical distance between the edges of the COCE grating bar and the edges of the inspection area may be estimated using the cortical magnification factor (M). The cortical magnification factor is often fitted to an equation of the form $M(r) = A(r + B)^{-C}$ [27,50]. The values reported by Sereno et al. [27] and used here were $A = 20.05$, $B = 0.08$ and $C = 1.26$ for visual area V1 and $A = 25.19$, $B = 0.09$ and $C = 1.53$ for visual area V2. The cortical distance d is then given by

$$\begin{aligned} d &= \int_{r_1}^{r_2} M(r) dr \\ &= \frac{A}{1-C} [(r_2 + B)^{1-C} - (r_1 + B)^{1-C}] \end{aligned} \quad (\text{A2})$$

where r_1 and r_2 are the eccentricities of the edges of the grating bar and the inspection area, respectively. Denoting the spatial frequency of the pattern by f_s and the diameter of the judgment area by j we have

$$r_1 = \frac{1}{4f_s} \quad \text{and} \quad r_2 = \frac{j}{2} \quad (\text{A3})$$

We make the approximation that the brightness signal must reach the edge of the inspection area within one half of the period T of the temporal modulation; filled-in brightness would be opposed by a reversal of edge contrast after this time. We use the edge of the area rather than the centre as our psychophysical criterion for brightness modulation was for modulation observed anywhere within the inspection area.

$$\frac{T}{2} = \frac{d}{v} \quad (\text{A4})$$

We then have the cut-off temporal frequency

$$f_t = \frac{v}{2d} \quad (\text{A5})$$

The cut-off temporal frequency can then be expressed as a function of spatial frequency by a combination of Eqs. (A2), (A3) and (A5).

$$f_t = \frac{v(1-C)}{2A \left[\left(\frac{1}{4f_s} + B\right)^{1-C} - \left(\frac{j}{2} + B\right)^{1-C} \right]} \quad (\text{A6})$$

References

- [1] O'Brien V. Contour perception, illusion and reality. *J Opt Soc Am* 1958;48:112–9.
- [2] Craik KJW. *The Nature of Psychology: A Selection of Papers, Essays and Other Writings*. Cambridge, MA: Cambridge University Press, 1966.
- [3] Cornsweet TN. *Visual Perception*. New York, NY: Academic Press, 1970.
- [4] Todorovic D. The Craik–O'Brien–Cornsweet effect: New varieties and their theoretical implications. *Perception Psychophys* 1987;42:545–60.
- [5] Marrocco RT, McClurkin JW, Young RA. Spatial summation and conduction latency classification of cells of the lateral geniculate nucleus of macaques. *J Neurosci* 1982;2:1275–91.
- [6] Derrington AM, Lennie P. Spatial and temporal contrast sensitivities of neurones in lateral geniculate nucleus of macaque. *J Physiol* 1984;357:219–40.
- [7] Gerrits HJM, Vendrik AJH. Simultaneous contrast, filling-in processes and information processing in Man's visual system. *Exp Brain Res* 1970;11:411–30.
- [8] Cohen MA, Grossberg S. Neural dynamics of brightness perception: Features, boundaries, diffusion and resonance. *Perception Psychophys* 1984;36:428–56.
- [9] Grossberg S, Todorovic D. Neural dynamics of 1-D and 2-D brightness perception: A unified model of classical and recent phenomena. *Perception Psychophys* 1988;43:241–77.
- [10] Campbell FW, Robson JG. Application of Fourier analysis to the visibility of gratings. *J Physiol* 1968;197:551–66.
- [11] Ratliff F, Sirovich L. Equivalence classes of visual stimuli. *Vis Res* 1978;18(7):845–51.
- [12] Sullivan GD, Georgeson MA. The missing fundamental illusion: Variation of spatio-temporal characteristics with dark adaptation. *Vis Res* 1977;17:977–81.
- [13] Campbell FW, Howell ER, Robson JG. The appearance of gratings with and without the fundamental Fourier component. *J Physiol (London)* 1971;217:17P–19.
- [14] Campbell FW, Howell ER, Johnstone JR. A comparison of threshold and suprathreshold appearance of gratings with components in the low and high spatial frequency range. *J Physiol* 1978;284:193–201.
- [15] Burr DC. Implications of the Craik–O'Brien illusion for brightness perception. *Vis Res* 1987;27(11):1903–13.
- [16] Kingdom F. Pattern discrimination with increment and decrement Craik–Cornsweet–O'Brien stimuli. *Spatial Vis* 1996;10:285–97.
- [17] McCourt ME. A spatial frequency dependent grating-induction effect. *Vis Res* 1982;22:119–34.
- [18] Tyrrell RA, Owens D. A new technique to rapidly assess the resting states of eyes and other threshold phenomena: The modified binary search (MOBS). *Behav Res Methods Instrum Comp* 1987;20:137–41.
- [19] Wahba, G. Spline models for observational data. In: CBMS-NSF Regional Conference Series in Applied Mathematics, vol. 59. Philadelphia, PA: Society for Industrial and Applied Mathematics, 1990.
- [20] Kelly DH. Motion and vision. II. Stabilized spatio-temporal threshold surface. *J Opt Soc Am* 1979;69:1340–9.
- [21] Rossi AF, Paradiso MA. Temporal limits of brightness induction and mechanisms of brightness perception. *Vis Res* 1996;36:1391–8.
- [22] Dooley RP, Greenfield MI. Measurements of edge-induced visual contrast and a spatial-frequency interaction of the Cornsweet illusion. *J Opt Soc Am* 1977;67:761–5.
- [23] Moulden B, Kingdom F. Light-dark asymmetries in the Craik–Cornsweet–O'Brien illusion and a new model of brightness coding. *Spatial Vis* 1990;5:101–28.
- [24] van den Brink G, Keemink CJ. Luminance gratings and edge effects. *Vis Res* 1976;16:155–9.
- [25] Sakata H. Mechanism of Craik–O'Brien effect. *Vis Res* 1981;21(5):693–9.
- [26] Grossberg S. Cortical dynamics of three-dimensional form, color and brightness perception: I. Monocular theory. *Perception Psychophys* 1987;41:87–116.
- [27] Sereno MI, Dale AM, Reppas JB, et al. Borders of multiple visual areas in humans revealed by functional magnetic resonance imaging. *Science* 1995;268:889–93.
- [28] Kanizsa G. Subjective contours. *Sci Am* 1976;234:51.
- [29] Petry S, Meyer GE. *The Perception of Illusory Contours*. New York, NY: Springer-Verlag, 1987.
- [30] Von der Heydt R, Peterhans E, Baumgartner G. Illusory contours and cortical neuron responses. *Science* 1984;224:1260–2.
- [31] Peterhans E, Von der Heydt R. Mechanisms of contour perception in monkey visual cortex. II. Contours bridging gaps. *J Neurosci* 1989;9:1749–63.
- [32] Von der Heydt R, Peterhans E. Mechanisms of contour perception in monkey visual cortex. I. Lines of pattern discontinuity. *J Neurosci* 1989;9:1731–48.
- [33] Hamada J. A multi-stage model for border contrast. *Biol Cybernetics* 1984;52:117–22.
- [34] Hamada J. Asymmetric lightness cancellation in Craik–O'Brien patterns of negative and positive contrast. *Biol Cybernetics* 1985;52:117–22.
- [35] Paradiso MA, Nakayama K. Brightness perception and filling-in. *Vis Res* 1991;31:1221–36.
- [36] Prince DA. Neurophysiology of epilepsy. *Annu Rev Neurosci* 1978;1:395–415.
- [37] Wyler AR, Ward AA. Neuronal firing patterns form epileptogenic foci of monkey and human. In: Delgado-Escueta AV, Ward AA, Woodbury DM, Porter RJ, editors. *Advances in Neurology. Basic Mechanisms of the Epilepsies: Molecular and Cellular Approaches*, vol. 44. New York: Raven Press, 1986:967–89.
- [38] Rockland KS, Lund JS. Intrinsic laminar lattice connections in primate visual cortex. *J Comp Neurol* 1983;216:303–18.
- [39] Martin KAC, Whitteridge D. Form, function and intracortical projections of spiny neurones in the striate visual cortex of the cat. *J Physiol (London)* 1984;353:463–504.
- [40] Blasdel GG, Lund JS, Fitzpatrick D. Intrinsic connections of macaque striate cortex: axonal projections of cells outside lamina 4C. *J Neurosci* 1985;5:3350–69.
- [41] Chapin JK, Sadeq M, Guise JLU. Corticocortical connections within the primary somatosensory cortex of the rat. *J Comp Neurol* 1987;263:326–46.
- [42] Gilbert CD, Hirsch JA, Wiesel TN. Lateral connections in the visual cortex. *Cold Spring Harbor Symposia on Quantitative Biology* 1990;55:663–77.
- [43] Wong RKS, Traub RD, Miles R. Cellular basis of neuronal synchrony in epilepsy. In: Delgado-Escueta AV, Ward AA, Woodbury DM, Porter RJ, editors. *Advances in Neurology. Basic Mechanisms of the Epilepsies: Molecular and Cellular Approaches*, vol. 44. New York, NY: Raven Press, 1986:583–92.
- [44] Chervin RD, Pierce PA, Connors BW. Periodicity and directionality in the propagation of epileptiform discharges across neocortex. *J Neurophysiol* 1988;60:1695–713.
- [45] Goldensohn ES, Salazar AM. Temporal and spatial distribution of intracellular potentials during generation and spread of epileptogenic discharges. In: Delgado-Escueta AV, Ward AA, Woodbury DM, Porter RJ, editors. *Advances in Neurology. Basic Mechanisms of the Epilepsies: Molecular and Cellular Approaches*, vol. 44. New York, NY: Raven Press, 1986:582–9.
- [46] Gutnick MJ, Wadman WJ. Intrinsic neuronal connectivity in neocortical brain slices as revealed by non-uniform propagation of paroxysmal discharges. *Soc Neurosci Abstr* 1986;12:349.

- [47] Wadman WJ, Gutnick MJ. Non-uniform propagation of epileptiform discharge in brain slices of rat neocortex. *Neuroscience* 1993;52:255–62.
- [48] De Valois RL, Webster MA, De Valois KK. Temporal properties of brightness and color induction. *Vis Res* 1986;26:887–97.
- [49] Arrington KF. The temporal dynamics of brightness filling-in. *Vis Res* 1994;34(24):3371–87.
- [50] Tootell RB, Silverman MS, Switkes E, De Valois RL. Deoxyglucose analysis of retinotopic organization in primate striate cortex. *Science* 1982;218:902–4.